Sánchez-Rivera, M.; Gozalbo, A.; Pérez-Herranz, V.; Mestre, S. (2020). Effect of pore generator on microstructure and resistivity of Sb2O3 and CuO doped SnO2 electrodes. Journal of Porous Materials. 27(6):1801-1808. https://doi.org/10.1007/s10934-020-00959-0

Effect of pore generator on microstructure and resistivity of Sb_2O_3 and CuO doped SnO_2 electrodes

M.-J. Sánchez-Rivera[a], A. Gozalbo[a,b] , V. Pérez-Herranz[c], S. Mestre[a,b]

a Instituto Universitario de Tecnología Cerámica, Universitat Jaume I, Castellón, Spain.

b Departamento de Ingeniería Química. Universitat Jaume I, Castellón, Spain.

c IEC Group, Departamento de Ingeniería Química y Nuclear, Universitat Politècnica de València, Spain.

e-mail address: mariajose.sanchez@itc.uji.es (M.-J. Sánchez-Rivera)

ABSTRACT

Sb_2O_3 and CuO doped SnO_2 ceramic electrodes could be an alternative to the ones currently used ones in the electrooxidation process of water pollutants. The rise of electrode surface by introducing a porogen agent on the composition was analysed in order to increase the electrochemical active surface. For this reason, several substances were tested. Although the densification and total pore volume had similar values, the microstructures and the pore size distributions generated were strongly dependent on porogen nature. A total of five porogens were tested, but petroleum coke turned out to be the best option for these electrodes. It was found that the electrical resistivity depends on the nature of pore generator. Furthermore, its relation to the porosity can be modelled with Archie's or Pabst's equations.

KEYWORDS

Electrode, Sintering, Porosity, Microstructure, Electrical conductivity

INTRODUCTION

One of the most important alternatives to eliminate water contaminants is the electrooxidation process. A chemical reaction takes place on the anode surface, generating hydroxyl radicals that allow the complete mineralization of organic pollutants [1]. However, the highly oxidizing environment requires anodes which withstand a chemical attack. Therefore, currently used electrodes are based on titanium oxides as well as tin-doped indium oxide [2], tin oxide doped with fluorine [3] or boron-doped diamond [4]. One of the main disadvantages of those electrodes is their high cost, either by the scarce elements that they include or by the expensive techniques needed for their manufacturing. Nevertheless, recent studies show that antimony and copper doped tin oxide electrodes processed by the traditional ceramic method can be a good option to replace the current anodes used in the electrooxidation process. In this way, recalcitrant and emergent contaminants from wastewaters can be removed [5].

The main component of the alternative electrode, tin oxide, is a n-type semiconductor used in a wide range of chemical and electronic applications [6–12]. Despite this, it is also recognized for its poor sinter ability [13]. It is the main drawback of its processing, although it is possible to improve their densification through some additives as ZnO, CeO_2 or In_2O_3 [14–16]. In a previous work, the authors tested copper oxide as sintering aid since many researchers had successfully tested it on SnO_2-based anodes used in the manufacture of aluminium [17–19]. The electrochemical characterization of this new ceramic electrode demonstrated that it fulfilled the needs of an anode for electrooxidation [20]. This electrode reached a high densification, and consequently a reduced open porosity. This fact constrained the electrochemical active surface, which is a critical parameter to improve its efficiency in electrooxidation processes. A network of interconnected pores can increase the contact area between the electrode and the effluent to be treated, and the simplest way to create it is to introduce a material that leaves voids after sintering.

Pore generators (also known as porogens) are frequently used in the synthesis of porous ceramics. They are substances which decomposes or oxidizes during the sintering thermal treatment creating these voids in the structure. Depending on the application and the process conditions, it can be an organic or inorganic compound. In addition, the porosity and the pore size distribution in the sintered specimen could be modified by varying the porogen type, its proportion or its properties (mainly particle size distribution). In the field of ceramic membranes [21,22], some renowned porogens are starch [23], polyethylene glycol [24], calcium carbonate [25] or kaolin [26]. A number of research studies have also shown that urea [27–29] can be used as a porogen agent, because it can increase the specific surface and also regulate the pore size distribution. In this way, generating some meso-pores which achieve a better electrochemical performance of the specimen. As a secondary effect, an increase in porosity theoretically will lead to an increase in the resistivity of the electrodes, nonetheless this phenomenon is difficult to model. Some equations have been proposed to relate porosity and electrical resistivity (or its inverse, the conductivity), but broad acceptance has not been attained yet.

This work has focused on the creation of porous Sb_2O_3 and CuO doped SnO_2 ceramic electrodes as the first requirement to increase their electrochemically active surface. At the same time, ceramic densification degree at the local level must be maintained in order to minimize the increase of electrical resistivity. Finally, a study of the effect of five pore generators (starch, ammonium nitrate, urea, ammonium carbonate and petroleum coke) on the microstructure and electrical properties of the electrodes was carried out. Starch is a quite common pore generator in ceramic experimentation. The other four were chosen owing to their low ash content after calcining and their different mechanical behaviour with respect to starch, with different degrees of similarity to a ceramic oxide. The effect of porosity over resistivity was measured. Furthermore, the viability of modelling the relationship between the two parameters with each of the proposed equations was evaluated.

EXPERIMENTAL PROCEDURE

Ceramic raw materials used in the synthesis of the electrodes were SnO_2 (purity 99.85 %, Quimialmel S.A., Spain), Sb_2O_3 as a dopant (purity 99.0 %, Alfa-Aesar, Germany) and CuO as a sintering aid (purity 97.0 %, Panreac S.A., Spain) in molar percentages of 97.8 mol.% of SnO_2, 1.0 mol.% of Sb_2O_3 and 1.2 mol.% of CuO respectively (reference composition R). Each one of the pore generators, starch (Roquette Freres S.A., France), NH_4NO_3 (purity ≥ 98.0 %, Sigma Aldrich, Spain), urea (99.0-100.5 %, Panreac S.A., Spain), $(NH_4)_2CO_3$ (Panreac S.A., Spain) and petroleum coke (British petroleum), was mixed with the ceramic fraction in 20/80 wt.% proportion. Every composition included as a ligand 0.8 wt.% of polivinylalcohol in addition (Mowiol 8-88, Clariant Iberica S.A. Spain). Table 1 shows the six compositions with the estimation of the volumetric fraction of porogen, calculated from the respective densities.

The ceramic raw materials were mixed using water as a fluid in a planetary mill working at 230 rpm for an hour (Pulverisette 5, Fritsch GmbH, Germany). The obtained suspension was dried in an oven at 110 ºC for 24 h. The dry powder was sieved through a 600 μm mesh and mixed with the pore generator. Those mixtures were dry-way prepared due to the high solubility of some porogen agents. A treatment of 30 s was used in an electric grinder with a constant speed. Every composition was moistened to 5.0% (kg water/kg dry solid) and prismatic specimens of 40x5x5 mm were shaped with a uniaxial manual press (Robima S.A., Spain), working at 250 $kg \cdot cm^{-2}$. Finally, the samples were sintered in a laboratory furnace (RHF1600, Carbolite Furnaces, UK) following specific thermal treatments designed to allow the complete decomposition or oxidation of the pore generator included in the specimen and to obtain samples which could be manipulated without fracture (Table 2).

Bulk density of green and sintered specimens was measured by mercury immersion (Archimedes' method). However, the data of green bulk density of the electrodes was calculated as the result of discounting the porogen content to the experimental value of green bulk density. The densification was calculated as the change in bulk density due to sintering divided by the change needed to attain a pore-free solid (according to German [30]). In other words, densification was referred only to the ceramic fraction, excluding porogens. The pore size distribution as well as the total pore volume and

characteristics pore diameters of the electrodes were measured through the mercury intrusion technique (AutoPore IV 9500, Micromeritics, USA) and the microstructure was visualized by FEG-SEM (QUANTA 200F, FEI Co, USA) in polished sections of selected samples. The electrical resistivity of sintered samples was measured with a resistance meter (RM 3545, Hioki E.E. Corp. Japan) by the four-points method, taking the average of ten measures for each specimen.

EXPERIMENTAL RESULTS AND DISCUSSION

1. Effects of porogens on processing

As expected, not all porogens were compatible with tin oxide processing. Starch and ammonium nitrate produced important defects during specimen's shaping, as cracks and laminations, which invalidated them after sintering for further studies. Firstly, starch is well known as an organic porogen agent that is broadly used in porous ceramic manufacture. However, their mechanical behaviour under pressing is very different from the SnO_2-based mixture. To be precise, the behaviour of starch along pressing causes many fissures that make the green samples very fragile. In addition, the sintering treatment generates specimens with plenty of cracks even though thermal cycle was adapted to facilitate a slow oxidation of starch. Secondly, the composition with ammonium nitrate could be shaped without too much difficulty. However, numerous efflorescences were observed on the surface of the specimens after drying, possibly due to the migration of the salt. In addition, sintered specimens lost uniformity and presented a very low densification and mechanical resistance, regardless of having adjusted the thermal cycle to allow a slow decomposition of ammonium nitrate before densification started. As it can be observed in figure 1, sintered samples obtained with these two porogens were easily broken. Consequently, starch and ammonium nitrate were considered inadequate porogens for the SnO_2-based electrodes, at least with the employed processing conditions.

Urea, ammonium carbonate and coke, showed a better behaviour throughout the process. The green samples could be manipulated without breaking. Only urea-containing specimens needed more care during shaping due to being more fragile. The compositions with ammonium carbonate and coke showed a similar behaviour to the porogen-free composition. In the case of the A composition, the high moisture value obtained after drying in the oven (27.8 % in comparation with 5.0 % and 4,1 % for compositions U and C respectively) indicates an almost complete decomposition of the ammonium carbonate together with the elimination of the water added to facilitate the pressing. Nevertheless, the sintering thermal treatment can cause the specimens to break under the pressure of the gases generated, considering that part of the porogen may be present in the specimens. If the complete decomposition of ammonium carbonate in the oven is confirmed, this porogen can be used in the future without modifying the sintering thermal cycle corresponding to the reference composition, shortening the process of obtaining porous electrodes.

2. Effect of porogens on bulk density, microstructure and pore size distribution

Bulk density of the shaped samples showed a decrease with respect to composition R as consequence of porogen addition to every composition (Figure 2). Nevertheless, the estimation of the bulk density discounting the porogen combined with the estimation of ceramic mixture's true density from the true densities of the three oxides (6.842 $g \cdot cm^{-3}$) allowed the calculation of the porosity of ceramic specimens excluding the porogen. This porogen-excluded green porosity of compositions U, A and C specimens were similar and around a 38% higher than the reference composition, that is coherent with the similar values of the estimated volume proportion of each porogen (Table 1). As a result, it was observed that the effect of the three porogens depended only slightly on their nature. After sintering, specimen's bulk density decreased from 6.696 $g \cdot cm^{-3}$ of reference composition to values between 4.395 $g \cdot cm^{-3}$ (composition U) and 3.998 $g \cdot cm^{-3}$ (composition A). Simultaneously, densification decreased from 95% to values in the 40-50% interval for the three porogen-containing specimens and porosity increased from 2% to around 40% (Figure 4). Therefore, ammonium carbonate is the most favourable compound to increase porosity, while urea is the one that increases it to a lesser extent and coke has an intermediate effect.

The appearance of the sintered electrodes was different for each of the compositions (Figure 3). Pores were nearly absent in the surface of reference specimens (composition R). In contrast, the other compositions generated specimens with a surface full of porosity, either with rounded pores, as in the case of compositions U and C, or in the form of cracks as it was the case with composition A. All the specimens had enough mechanical strength to freely manipulate them and carry out their characterization. The differences in appearance were reflected in the microstructures, as SEM images show (Figure 3). Composition R specimens possessed a microstructure of a few, small and rounded pores, characteristic of the last stage of sintering. By contrast, ammonium carbonate and urea generate big pores with irregular shapes, probably related to the geometry of the porogen's particles, dispersed in a matrix which showed a high degree of densification at local level. Obviously, the big pores created by the porogen are not eliminated along the sintering thermal cycle. On the other hand, coke generated a completely different microstructure. Instead of a dense microstructure where large pores are randomly distributed, a microporous microstructure was obtained, with a small proportion of denser zones (possible agglomerates present in the mix of raw materials given their rounded shape). This result means that particle size distribution of coke was displaced to lower diameters with respect to ammonium carbonate and urea, and it also seems that coke is easier to mix with the ceramic raw materials under the employed mixing parameters.

The characteristics of sample's microstructure was confirmed by the pore size distribution measurements (Figure 5). Compositions A and U specimens had a very similar pore size distribution but displaced to a little bigger diameter for the specimens processed with urea. Those distributions are not sigmoidal and pores with diameters bigger than 10 microns are the majority. By contrast, the pore size distribution created by the coke is approximately sigmoidal and centred around a diameter of 3 microns. On the other hand, the two sets of total pore volume data (measured by mercury intrusion and calculated from the difference between the estimated true density and the measured bulk density), allow the estimation of the proportion of closed porosity (Table 3). As expected, nearly all the porosity is closed in composition R specimens. In fact, every porogen generates different proportions of closed porosity. Ammonium carbonate is the porogen which generates a higher proportion of closed porosity and coke is the one which generates a nearly completely open porosity, while urea generates an intermediate proportion of closed porosity.

3. Effect of porogens on resistivity

The direct consequence of porosity is a decrease in electrode's electrical conductivity, as expected (Table 4). In particular, an increase of approximately three orders of magnitude was experienced when a 20 wt.% of porogen was included in the reference composition, whose consequence was a volume fraction of pores around 40%.

Some equations proposed in the bibliography has been tested to model the relation between the conductivity of pore-free material (σ_0), the porosity (ε) and the conductivity of the porous material (σ), or its inverse the resistivity (ρ).

1) Archie's empirical equation (Eq.1) proposes a potential relationship where **m** is theArchie's exponent, which is related to the connectivity between the nonconducting phase (pores) and the conducting one (ceramic) [31].

$$\sigma = \sigma_0(1-\varepsilon)^m \quad \text{Eq.1}$$

2) Wagner equation (Eq. 2), [32].

$$\sigma \propto \sigma_0(1-\varepsilon) \quad \text{Eq.2}$$

3) The Maxwell-Garnett model (Eq.3) and the Bruggeman approximation (Eq.4) were derived from Effective Medium Theory (EMT), which considers spherical inclusions in the matrix. [33].

$$\sigma = \sigma_0 \frac{1-\varepsilon}{1+0.5\varepsilon} \quad \text{Eq.3}$$

$$\sigma = \sigma_0 \frac{2-3\varepsilon}{2} \quad \text{Eq.4}$$

4) The Sun et al.'s equation considers that the effect of porosity varies depending on whether it is closed or open [34]. In this model the resistivity (ρ) of a solid with a volume fraction w_1 of closed porosity and a volume fraction w_2 of open porosity is given by Eq. 5, considering ρ_0 the resistivity of pore-free solid and x and y the fractions of open and closed porosity (x+y = 1).

$$\rho = \rho_0 \frac{\frac{16+13.75w_1}{(4+4w_1)^2}\cdot\frac{4+5.46w_2}{(2-1.91w_2)^2}}{x\frac{16+13.75w_1}{(4+4w_1)^2}+y\frac{4+5.46w_2}{(2-1.91w_2)^2}} \qquad \text{Eq.5}$$

5) Pabst's exponential relation, which introduces the parameter κ, is a simplified version of their more complex model which entails spheroidal pores with different aspect ratios and orientations [35].

$$\sigma = \sigma_0 exp\left(-\frac{\kappa\varepsilon}{1-\varepsilon}\right) \quad \text{Eq.6}$$

The proposed models do not predict the strong variation in resistivity in function of porosity obtained in our specimens (Figure 6). Only Archie's equation and Pabst's exponential equation gives an approximation but for high values of their respective parameter. To be precise, Archie's equation estimates the order of magnitude of the change in conductivity if the value of **m** is higher than ten, which is superior to values obtained for correlations of ionic conductivity-porosity in $La_2Mo_{1.5}W_{0.5}O_9$, YSZ, $Ce_{0.9}Gd_{0.1}O_{1.95}$ and $La_{9.6}Ge_{5.5}Al_{0.5}O_{26.15}$ which were 2.69, 2.74, 1.9 and 1.8 respectively [33]. In the case of **k** parameter of exponential equation, Pabst et al. deduced that this parameter could tend to infinity if the pores were in the form of randomly oriented disks, and the thickness could tend to zero [35], giving a possible interpretation of the obtained data. In addition, the experimental data for the three groups of samples cannot be modelled with a single pair of values for each model, meaning that porogen nature could also play a role over conductivity. The calculated values of the parameters of Archie and Pabst's equations for the three groups of samples pointed to a similar value of ρ_0 for the porous-free sample (around 5.4 Ω·cm for Archie's equation and 5.1 Ω·cm for the Pabst's equation, Table 4), which was coherent with the identical nature of the ceramic matrix. However, the values of the second parameter showed notable differences, spanning from 10.8 to 15.9 in the case of **m** and from 8.0 to 12.5 in the case of **k**.

Assuming that parameter **m** is related to connectivity of the conductive phase, differences found in the calculated values would mean that in the Sb_2O_3 and CuO doped SnO_2 ceramic electrodes the connectivity of the paths for the transfer of the electrons is much lower than that which would be deduced from the microstructure, especially in the samples of compositions A and U. By contrast, samples of composition C would have a microstructure more in accordance with the value of **m**, even though its value is intermediate between the other two compositions. According to the Pabst et al. model, the shape of the pores should resemble finely oriented random discs, but only samples of composition C could approximate this estimate. These results seem to indicate that in samples A and U not all the ceramic phase actually is a path for charge carriers, but only a fraction of it. As a hypothesis, it could be suggested that gases generated by decomposition of urea and ammonium carbonate particles along sintering thermal treatment reduced the proportion of charge carriers in their surroundings, leaving a much more reduced network of paths for charge carriers. However, to the best of our knowledge, no data has been published showing the same behaviour in other electrically conductive ceramics.

CONCLUSIONS

It has been demonstrated the viability of obtaining porous ceramic electrodes through the traditional ceramic method starting from a CuO-Sb_2O_3-SnO_2 composition with addition of a porogen. Nevertheless, the porogen must be selected considering its behaviour along the process. Firstly, the dry pressing shaping requires porogens with mechanical behaviour close to the ceramic matrix, which excludes materials as starches. Secondly, the drying stage prevents the use of salts that easily generate efflorescences, such as ammonium nitrate. Finally, the heat treatments designed to sinter the electrodes

must include stages to slowly decompose/oxidize the selected porogen. Urea, ammonium carbonate or petroleum coke satisfy the above requirements.

The values for bulk density, densification and total pore volume were in the same order of magnitude for the sintered samples obtained with urea, ammonium nitrate or petroleum coke as porogen, when added in a 20 wt.% proportion. However, microstructure and pore size distribution were strongly dependent of porogen nature. Urea and ammonium nitrate generate a microstructure of big pores partially connected, whereas petroleum coke generates a more homogeneous microstructure of smaller pores and fully connected. Therefore, it is possible to have a certain degree of control over the microstructure through an adequate selection of porogen.

Electrical resistivity increases with porosity, but the magnitude of the change can only be modelled with Archie's or Pabst's equations. Both equations estimate similar values of the resistivity for the pore-free electrode, although the parameters related to the microstructure take abnormally high values in the case of urea and ammonium carbonate. These values could be interpreted considering that not all the ceramic matrix intervenes in the transfer of charge carriers. The cause would be that some processes related to urea or ammonium carbonate behaviour along the thermal cycle reduce the conductivity of the ceramic matrix fraction closest to them. As a direct result, petroleum coke seems to be a good material to create porosity in Sb_2O_3 and CuO doped SnO_2 ceramic electrodes processed by the traditional ceramic method.

ACKNOWLEDGEMENTS

The authors are very grateful to the Ministerio de Economia y Competitividad (Projects: CTQ2015-65202-C2-1-R and CTQ2015-65202-C2-2-R) and to the European Regional Development Fund (FEDER), for their economic support.

REFERENCES

[1] C.A. Martínez-Huitle, S. Ferro, Electrochemical oxidation of organic pollutants for the wastewater treatment: direct and indirect processes, Chem. Soc. Rev. 35 (2006) 1324–1340. doi:10.1039/B517632H.

[2] C.A. Kent, J.J. Concepcion, C.J. Dares, D.A. Torelli, A.J. Rieth, A.S. Miller, P.G. Hoertz, T.J. Meyer, Water oxidation and oxygen monitoring by cobalt-modified fluorine-doped tin oxide electrodes, J. Am. Chem. Soc. 135 (2013) 8432–8435. doi:10.1021/ja400616a.

[3] M.P. Miranda, R. Del Rio, M.A. Del Valle, M. Faundez, F. Armijo, Use of fluorine-doped tin oxide electrodes for lipoic acid determination in dietary supplements, J. Electroanal. Chem. 668 (2012) 1–6. doi:10.1016/j.jelechem.2011.12.022.

[4] M.A.Q. Alfaro, S. Ferro, C.A. Martínez-Huitle, Y.M. Vong, Boron doped diamond electrode for the wastewater treatment, J. Braz. Chem. Soc. 17 (2006) 227–236. doi:10.1590/S0103-50532006000200003.

[5] J. Mora-Gómez, M. García-Gabaldón, E. Ortega, M.-J. Sánchez-Rivera, S. Mestre, V. Pérez-Herranz, Evaluation of new ceramic electrodes based on Sb-doped SnO 2 for the removal of emerging compounds present in wastewater, Ceram. Int. 44 (2018) 2216–2222. doi:10.1016/j.ceramint.2017.10.178.

[6] C.J. Evans, Industrial uses of tin chemicals, in: Chem. Tin, Springer Netherlands, Dordrecht, 1998: pp. 442–479. doi:10.1007/978-94-011-4938-9_12.

[7] J. Molera, T. Pradell, N. Salvadó, M. Vendrell-Saz, Evidence of Tin Oxide Recrystallization in Opacified Lead Glazes, J. Am. Ceram. Soc. 82 (2004) 2871–2875. doi:10.1111/j.1151-2916.1999.tb02170.x.

[8] P.P. Tsai, I.-C. Chen, M.H. Tzeng, Tin oxide (SnOX) carbon monoxide sensor fabricated by thick-film methods, Sensors Actuators B Chem. 25 (1995) 537–539. doi:10.1016/0925-4005(95)85116-X.

[9] F. Li, J. Xu, X. Yu, L. Chen, J. Zhu, Z. Yang, X. Xin, One-step solid-state reaction synthesis and gas sensing property of tin oxide nanoparticles, Sensors Actuators B …. 81 (2002) 165–169. http://www.sciencedirect.com/science/article/pii/S0925400501009479.

[10] S. Zuca, M. Terzi, M. Zaharescu, K. Matiasovsky, Contribution to the study of SnO2-based ceramics, J. Mater. Sci. 26 (1991) 1673–1676. doi:10.1007/BF00544681.

[11] M. BATZILL, U. DIEBOLD, The surface and materials science of tin oxide, Prog. Surf. Sci. 79 (2005) 47–154. doi:10.1016/j.progsurf.2005.09.002.

[12] G. Monrós, El color de la cerámica : nuevos mecanismos en pigmentos para los nuevos procesados de la industria cerámica, n.d. https://books.google.es/books/about/El_Color_de_la_cerámica.html?id=yfIogcGvdqUC&redir_esc=y (accessed August 29, 2018).

[13] E.R. Leite, J.A. Cerri, E. Longo, J.A. Varela, C.A. Paskocima, Sintering of ultrafine undoped SnO2 powder, J. Eur. Ceram. Soc. 21 (2001) 669–675. doi:10.1016/S0955-2219(00)00250-8.

[14] S. Mihaiu, O. Scarlat, G. Aldica, M. Zaharescu, SnO2 electroceramics with various additives, J. Eur. Ceram. Soc. 21 (2001) 1801–1804. doi:10.1016/S0955-2219(01)00119-4.

[15] C.R. Foschini, L. Perazolli, J.A. Varela, Sintering of tin oxide using zinc oxide as a densification aid, J. Mater. Sci. 39 (2004) 5825–5830. doi:10.1023/B:JMSC.0000040095.03906.61.

[16] M.S. Castro, C.M. Aldao, Characterization of SnO2-varistors with different additives, J. Eur. Ceram. Soc. 18 (1998) 2233–2239. doi:10.1016/S0955-2219(97)00130-1.

[17] A.-M. Popescu, S. Mihaiu, S. Zuca, Microstructure and Electrochemical Behaviour of some SnO2-based Inert Electrodes in Aluminium Electrolysis, Zeitschrift Für Naturforsch. A. 57 (2002) 71–75. doi:10.1515/zna-2002-1-210.

[18] M.R. Sahar, M. Hasbullah, Properties of SnO2-based ceramics, 30 (1995) 5304–5305.

[19] D. Nisiro, G. Fabbri, G.C. Celotti, A. Bellosi, Influence of the additives and processing conditions on the characteristics of dense SnO2-based ceramics, J. Mater. Sci. 38 (2003) 2727–2742. doi:10.1023/A:1024459307992.

[20] M.-J. Sánchez-Rivera, CuO improved (Sn,Sb)O2 ceramic anodes for electrochemical advanced oxidation processes, Int. J. Appl. Ceram. Technol. (2018).

[21] B. Das, B. Chakrabarty, P. Barkakati, Preparation and characterization of novel ceramic membranes for micro-filtration applications, Ceram. Int. 42 (2016) 14326–14333. doi:10.1016/j.ceramint.2016.06.125.

[22] I. Hedfi, N. Hamdi, M.A. Rodriguez, E. Srasra, Development of a low cost micro-porous ceramic membrane from kaolin and Alumina, using the lignite as porogen agent, Ceram. Int. 42 (2016) 5089–5093. doi:10.1016/j.ceramint.2015.12.023.

[23] M. García-Gabaldón, V. Pérez-Herranz, E. Sánchez, S. Mestre, Effect of porosity on the effective electrical conductivity of different ceramic membranes used as separators in eletrochemical reactors, J. Memb. Sci. 280 (2006) 536–544. doi:10.1016/j.memsci.2006.02.007.

[24] J.-H. Kim, K.-H. Lee, Effect of PEG additive on membrane formation by phase inversion, J. Memb. Sci. 138 (1998) 153–163. doi:10.1016/S0376-7388(97)00224-X.

[25] B.K. Nandi, R. Uppaluri, M.K. Purkait, Preparation and characterization of low cost ceramic membranes for micro-filtration applications, Appl. Clay Sci. 42 (2008) 102–110.

doi:10.1016/j.clay.2007.12.001.

[26] F. Bouzerara, A. Harabi, S. Condom, Porous ceramic membranes prepared from kaolin, Desalin. Water Treat. 12 (2009) 415–419. doi:10.5004/dwt.2009.1051.

[27] Q. Guibao, L. Tengfei, W. Jian, B. Chenguang, Preparation of Titanium Foams with Uniform and Fine Pore Characteristics Through Powder Metallurgy Route Using Urea Particles as Space Holder, in: Springer, Cham, 2018: pp. 861–868. doi:10.1007/978-3-319-72526-0_82.

[28] K. Zou, Y. Deng, J. Chen, Y. Qian, Y. Yang, Y. Li, G. Chen, Hierarchically porous nitrogen-doped carbon derived from the activation of agriculture waste by potassium hydroxide and urea for high-performance supercapacitors, J. Power Sources. 378 (2018) 579–588. doi:10.1016/j.jpowsour.2017.12.081.

[29] S. Vijayan, R. Narasimman, K. Prabhakaran, A urea crystal templating method for the preparation of porous alumina ceramics with the aligned pores, J. Eur. Ceram. Soc. 33 (2013) 1929–1934. doi:10.1016/j.jeurceramsoc.2013.02.031.

[30] R.M. German, Sintering theory and practice, John Wiley & Sons, Inc, 1996.

[31] G.E. Archie, The Electrical Resistivity Log as an Aid in Determining Some Reservoir Characteristics, Trans. AIME. 146 (1942) 54–62.

[32] P. WAGNER, J.A. O'ROURKE, P.E. ARMSTRONG, Porosity Effects in Polycrystalline Graphite, J. Am. Ceram. Soc. 55 (1972) 214–219. doi:10.1111/j.1151-2916.1972.tb11262.x.

[33] H. El Khal, A. Cordier, N. Batis, E. Siebert, S. Georges, M.C. Steil, Effect of porosity on the electrical conductivity of LAMOX materials, Solid State Ionics. 304 (2017) 75–84. doi:10.1016/j.ssi.2017.03.028.

[34] S. Tian-Ming, D. Li-Min, W. Chen, G. Wen-Li, W. Li, T.-X. Liang, NEW CARBON MATERIALS Effect of porosity on the electrical resistivity of carbon materials, New Carbon Mater. 28 (2013) 349–354. doi:10.1016/S1872-5805(13)60087-6.

[35] W. Pabst, E. Gregorová, Conductivity of porous materials with spheroidal pores, J. Eur. Ceram. Soc. 34 (2014) 2757–2766. doi:10.1016/j.jeurceramsoc.2013.12.040.

APPENDIX

Tables:

Table 1: Tested compositions (in wt.%).

composition	ceramic			porogen		PVA	Estimated porogen volume (%)
	SnO_2	Sb_2O_3	CuO	type	wt.%		
R	97.48	1.93	0.59	-	-	0.80	-
S	77.95	1.55	0.50	Starch	20	0.80	26.0
AN	77.95	1.55	0.50	NH_4NO_3	20	0.80	11.6
U	77.95	1.55	0.50	Urea	20	0.80	15.2
A	77.95	1.55	0.50	$(NH_4)_2CO_3$	20	0.80	13.3
C	77.95	1.55	0.50	coke	20	0.80	14.8

Table 2: Sintering thermal treatments used with every composition (T_0 = initial temperature, r_i = heating rate of stage i, T_i = final temperature of stage i, t_i = soaking time at the final temperature of stage i).

Parameter	Pore generator included on the composition					
	None	Starch	NH_4NO_3	$(NH_4)_2CO_3$	Urea	Coke
T_0 (ºC)	25	25	25	25	25	25
r_1 (ºC·min^{-1})	15	10	10	1	1	10
T_1 (ºC)	1200	200	200	200	300	200
t_1 (min)	360	60	60	60	0	60
r_2 (ºC·min^{-1})	Natural cooling	1	0.5	15	2	1
T_2 (ºC)		300	300	1200	400	300
t_2 (min)		60	60	360	0	60
r_3 (ºC·min^{-1})		1	15	Natural cooling	15	1
T_3 (ºC)		500	1300		1200	500
t_3 (min)		60	360		360	60
r_4 (ºC·min^{-1})		15	Natural cooling		Natural cooling	15
T_4 (ºC)		1200				1200
t_4 (min)		360				360
		Natural cooling				Natural cooling

Table 3: Results of the mercury intrusion assay and estimations of total pore volume, from the bulk density, and the fraction of closed porosity.

Reference	Mercury intrusion assay				Estimation	
	Total pore volume ($cm^3 \cdot g^{-1}$)	D_{10} (µm)	D_{50} (µm)	D_{90} (µm)	Total pore volume ($cm^3 \cdot g^{-1}$)	Closed pores (%)
R	0.0003	147.7	25.7	7.4	0.003	92.2
U	0.0698	115.8	28.0	1.5	0.081	14.2
A	0.0757	99.1	12.2	0.9	0.104	27.1
C	0.0957	5.6	3.5	1.7	0.099	3.5

Table 4: Calculated parameters of Archie's and Pabst's equations.

Composition	Resistivity	Archie's equation		Pabst's equation	
	ρ (Ω·cm)	ρ_0 (Ω·cm)	m (-)	ρ_0 (Ω·cm)	k (-)
U	197.6	5.7	15.9	5.3	12.5
A	60.9	5.1	10.7	4.8	8.0
C	142.4	5.4	12.8	5.0	9.7

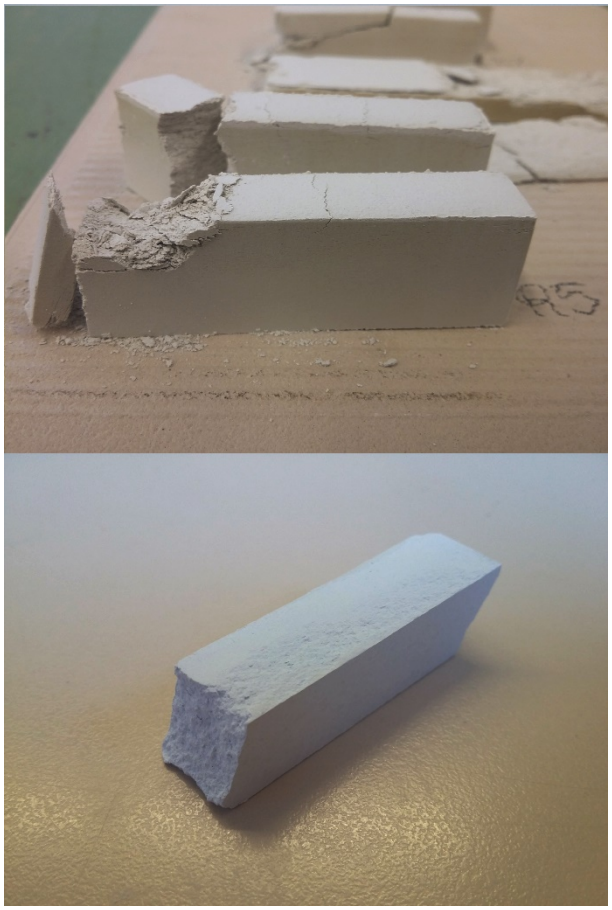

Figure 1. Sintered electrodes which included starch (upper) and NH_4NO_3 (down) as porogens.

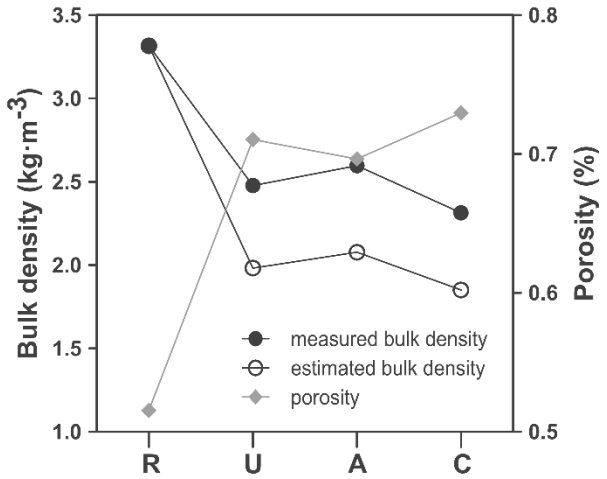

Figure 2. Experimental bulk density of green dry-pressed specimens and estimated values of their bulk density and porosity after discounting the mass and volume of the porogen.

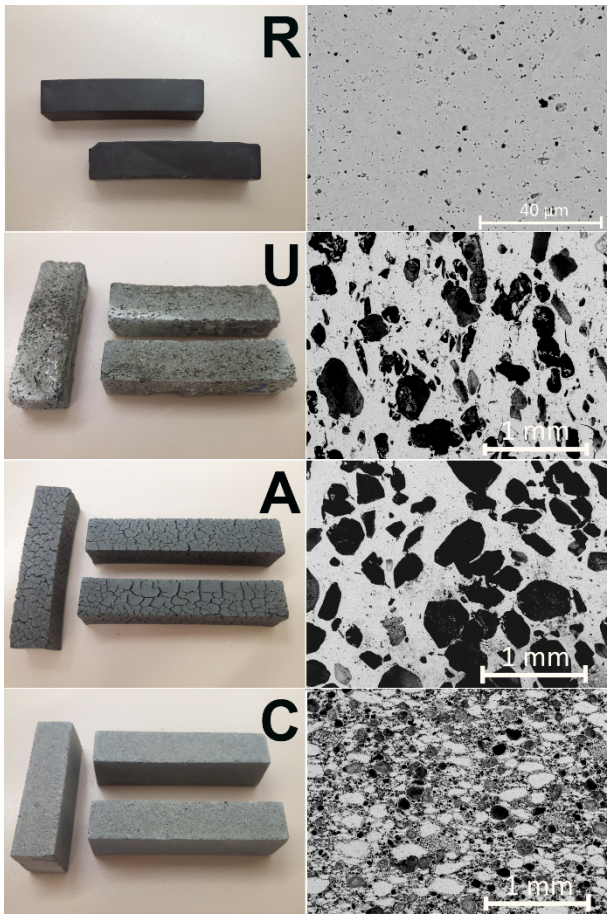

Figure 3. Visual appearance and micrographs of the sintered electrodes. R: base composition without porogen; U: composition with 20 wt.% of urea; A: composition with 20 wt.% of ammonium carbonate; C: composition with 20 wt.% of petroleum coke.

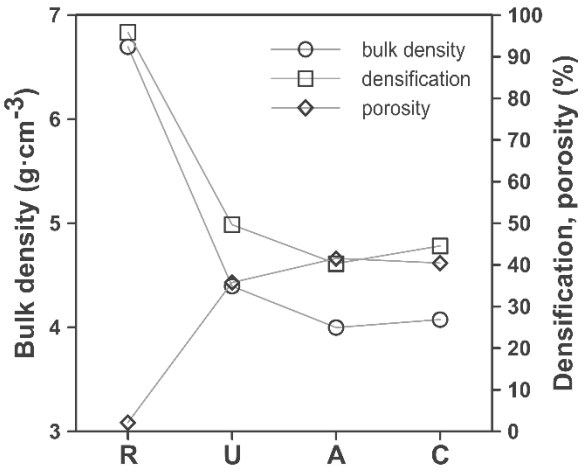

Figure 4. Bulk density, densification and estimated porosity of the sintered specimens.

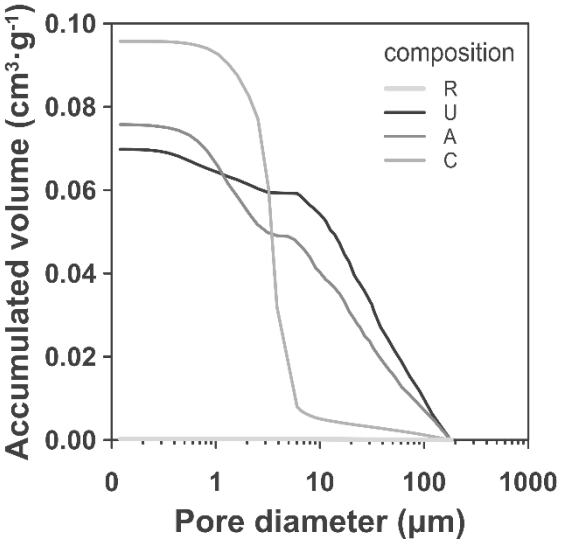

Figure 5. Pore size distribution of the sintered specimens.

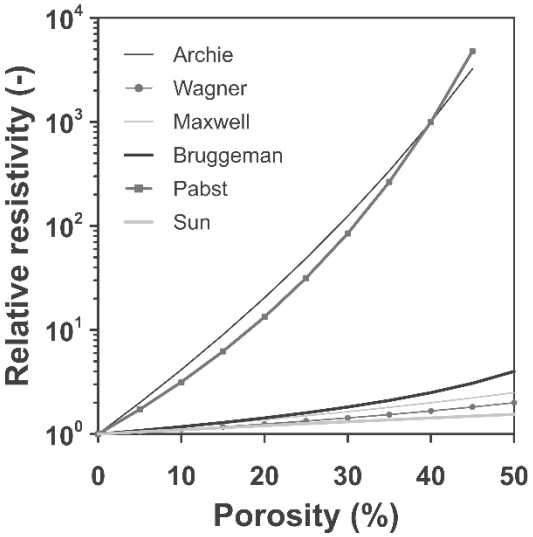

Figure 6. Calculated evolution of resistivity as a function of porosity according to six equations proposed in the bibliography. Whenever possible, real parameters of the samples have been used.